Electronic Supplementary Material (ESI) for New Journal of Chemistry.
This journal is © The Royal Society of Chemistry and the Centre National de la Recherche Scientifique 2023

Journal Name

ARTICLE TYPE

Cite this: DOI: 00.0000/xxxxxxxxxx

Electronic Supplementary Information(ESI) of "Evidence of Half-metallicity at the $BiFeO_3$(001) surface"

Soumyasree Jena,[a] Sanjoy Datta,*[a,b]

Received Date
Accepted Date

DOI: 00.0000/xxxxxxxxxx

DOS and LDOS corresponding to BiO termination

In Figs.1 and 2, the layered density of states (DOS) for 4L and 6L thick BiO terminated surfaces are presented. Except structure-II, metallic states are prominent for all the structures. The spin-down channels corresponding to bottom two layers are insulating, which is shown in fig.1(b). The top-layer spin-down channels are conducting. However, the contribution is less as compared to other structures. In case 6L thick structure-II, the half-metallicity is destroyed due to the tiny contribution from spin-down channel in bottom-layer. Furthermore, the local density of states (LDOS) corresponding to structure-II, is presented in fig.3.

Local density of states (LDOS)

The 2DHG is destroyed in the case of 6L thick surfaces for structure-III and IV. To understand the orbital contribution in these cases, we have studied the local density of states for structure-III and structure-IV. The results are presented in Fig. 4. In all the cases, along with the Fe-3d and O-2p orbital contributions, the role of Bi-6p is also found.

Oxygen vacancy

In this section, we have carried out a brief study of the effect of oxygen vacancy on the electronic properties of the surface states in this structure. In Fig. 5, we have indicated the two inequivalent oxygen sites at the top layer of a 4L thick surface. The vacancies are generated at either of these two inequivalent positions, which are named 'V1' and 'V2'. In Figs. 6 and 7, we have presented the individual layer resolved DOS up to 3ml thick surface layers. It is evident from these results that having oxygen vacancy at the top surface leads to the destruction of the 2DHG at the surface layers.

Full-slab-study

In this section, the FeO_2 terminated slabs with thicknesses of 4L and 8L are presented. The DOS and LDOS results for full slab geometries where the whole slab structures have been allowed to relax before investigating the electronic properties are presented. For a 4L thick slab, half-metallic electronic state and 2DHG have been found to persist in all the structures except structure-I. Surprisingly, structure-I turns out to be metallic in this case. The layer resolved DOS for each structure is presented in Fig. 8. From Fig. 8(a), it is evident that although the top surface of structure-I still exhibits half-metallicity, the bottom layer shows metallic character. However, it is evident that only one spin channel contributes to the Fermi energy for the rest of the structures.

Furthermore, it is also clear that the charge carriers are hole types in these structures. Surprisingly, however, for a 8L thick slab, the structure-I turns out to be a half-metal (Fig. 10(a)). However, from the thermodynamic stability analysis (Table 5), we find that the surface energy of this structure is negative, which indicates that this structure might not be stable. In the case of structure-II, which is thermodynamically most stable, a tiny contribution of spin-down electron carriers from the third FeO_2 layer destroys the half-metallic character. In addition, structure-I and II still exhibit the existence of 2DHG. The 2DHG ceases to exist in structures III and IV. From Figs. 10(c) and (d), it is evident that structures III and IV behave as metals. To understand the orbital contribution of each structure, we have also presented the LDOS results for the 4L and 8L thick slabs in Figs. 9 and 11. From the LDOS results, we observe that Bi does not contribute to the Fermi energy, except for a 4L thick slab of structure-I and 8L thick structure-IV, which are metallic in nature, while contributions from $Fe-3d$ and $O-2p$ orbitals are found in both the half-metallic and metallic cases. From the LDOS results (Fig. 11(b)

[a] *Department of Physics and Astronomy, National Institute of Technology, Rourkela, Odisha, India, 769008; E-mail: jenasoumyasree@gmail.com*
[b] *Center for Nanomaterials, National Institute of Technology, Rourkela, Odisha, India, 769008;E-mail:dattas@nitrkl.ac.in*

† Electronic Supplementary Information (ESI) available: [details of any supplementary information available should be included here]. See DOI: 00.0000/00000000.

‡ Additional footnotes to the title and authors can be included *e.g.* 'Present address:' or 'These authors contributed equally to this work' as above using the symbols: ‡, §, and ¶. Please place the appropriate symbol next to the author's name and include a `\footnotetext` entry in the the correct place in the list.

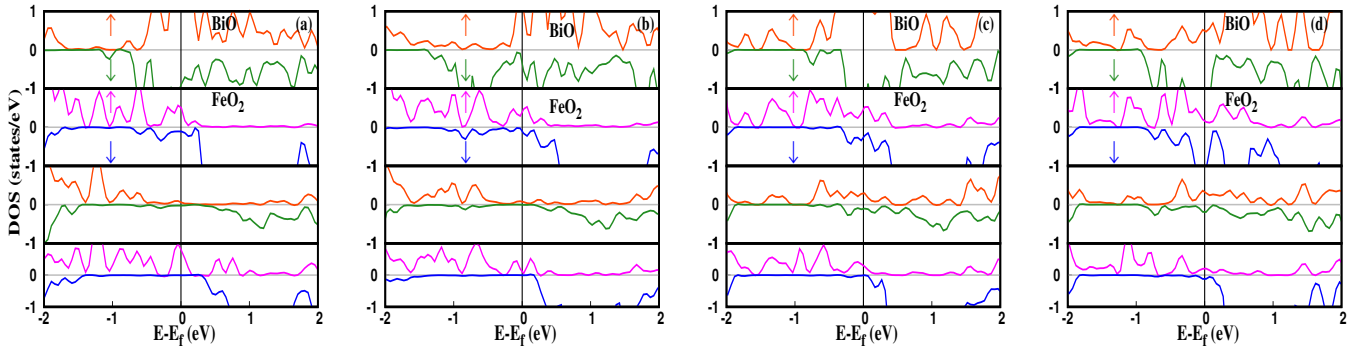

Fig. 1 Density of states (DOS) of 4L slab-thicknesses with BiO termination for (a) structure-I, (b) structure-II, (c) structure-III, and (d) structure-IV respectively.

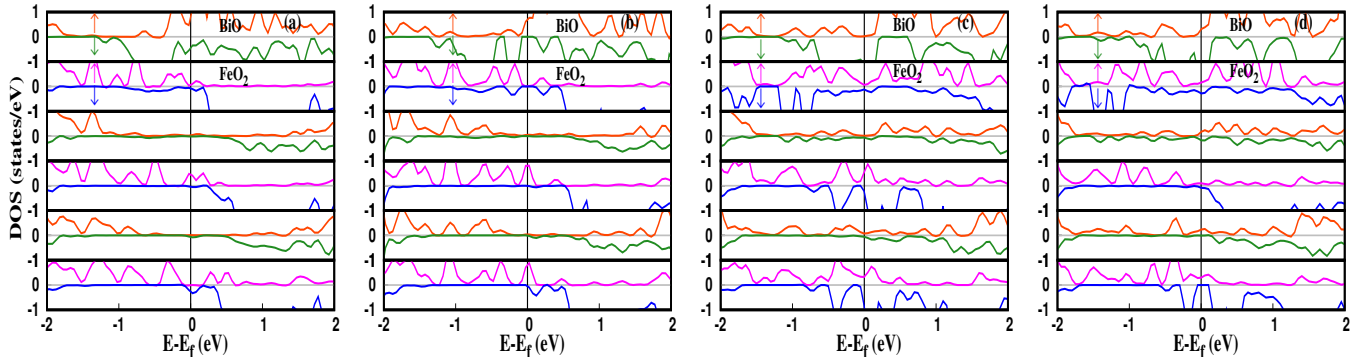

Fig. 2 Layered density of states (DOS) of 6L surface-thicknesses with BiO termination (a) structure-I, (b) structure-II, (c) structure-III, and (d) structure-IV respectively.

Table 1 q_{Fe}, q_O, q_{Bi} are Bader's topological charges corresponding to iron (Fe), oxygen (O), and bismuth (Bi) respectively for the FeO_2 and BiO terminations of structure-II.

Layer-No.	FeO_2	BiO
	Two-layers (2L)	
L1	q_{Fe} = 1.48, q_O = -1.18, q_{tot} = -0.88	q_{Bi} = 1.05, q_O = -1.15, q_{tot} = -0.10
L2	q_{Bi} = 1.78, q_O = -1.23, q_{tot} = 0.55	q_{Fe} = 1.76, q_O = -1.18, q_{tot} = -0.61
L3	q_{Fe} = 1.75, q_O = -1.20, q_{tot} = -0.65	q_{Bi} = 1.82, q_O = -1.24, q_{tot} = 0.58
L4	q_{Bi} = 1.96, q_O = -0.97, q_{tot} = 0.99	q_{Fe} = 1.71, q_O = -0.78, q_{tot} = 0.15
	Four-layers (4L)	
L1	q_{Fe} = 1.41, q_O = -1.17, q_{tot} = -0.93	q_{Bi} = 0.91, q_O = -1.12, q_{tot} = -0.21
L2	q_{Bi} = 1.83, q_O = -1.19, q_{tot} = 0.64	q_{Fe} = 1.77, q_O = -1.20, q_{tot} = -0.63
L3	q_{Fe} = 1.77, q_O = -1.20, q_{tot} = -0.63	q_{Bi} = 1.84, q_O = -1.18, q_{tot} = 0.66
L4	q_{Bi} = 1.84, q_O = -1.22, q_{tot} = 0.62	q_{Fe} = 1.77, q_O = -1.20, q_{tot} = -0.63
L5	q_{Fe} = 1.75, q_O = -1.21, q_{tot} = -0.67	q_{Bi} = 1.81, q_O = -1.26, q_{tot} = 0.55
L6	q_{Bi} = 1.94, q_O = -1.22, q_{tot} = 0.72	q_{Fe} = 1.72, q_O = -1.22, q_{tot} = -0.72
L7	q_{Fe} = 1.65, q_O = -1.19, q_{tot} = -0.73	q_{Bi} = 1.95, q_O = -1.18, q_{tot} = 0.77
L8	q_{Bi} = 1.99, q_O = -1.02, q_{tot} = 0.97	q_{Fe} = 1.75, q_O = - 0.78, q_{tot} = 0.19
	Six-layers (6L)	
L1	q_{Fe} = 1.49, q_O = -1.16, q_{tot} = -0.83	q_{Bi} = 0.88, q_O = -1.13, q_{tot} = -0.25
L2	q_{Bi} = 1.79, q_O = -1.21, q_{tot} = 0.58	q_{Fe} = 1.78, q_O =-1.2, q_{tot} = -0.62
L3	q_{Fe} = 1.80, q_O = -1.21, q_{tot} = -0.62	q_{Bi} = 1.85, q_O = -1.19, q_{tot} = 0.66
L4	q_{Bi} = 1.84, q_O = -1.20, q_{tot} = 0.64	q_{Fe} = 1.78, q_O = -1.20, q_{tot} = -0.62
L5	q_{Fe} = 1.78, q_O = -1.22, q_{tot} = -0.66	q_{Bi} = 1.85, q_O= -1.20, q_{tot} = 0.65
L6	q_{Bi} = 1.83, q_O = -1.25, q_{tot} = 0.58	q_{Fe} = 1.79, q_O = -1.2, q_{tot} = -0.61
L7	q_{Fe} = 1.76, q_O = -1.22, q_{tot} = -0.68	q_{Bi} = 1.80, q_O = -1.24, q_{tot} = 0.56
L8	q_{Bi} = 1.91, q_O = -1.21, q_{tot} = 0.70	q_{Fe} = 1.69, q_O = -1.22, q_{tot} = -0.75
L9	q_{Fe} = 1.71, q_O = -1.21, q_{tot} = -0.71	q_{Bi} = 1.92, q_O =-1.19, q_{tot} = 0.73
L10	q_{Bi} = 1.92, q_O = -1.19, q_{tot} = 0.73	q_{Fe} = 1.71, q_O =-1.22, q_{tot} = -0.73
L11	q_{Fe} = 1.67, q_O = -1.19, q_{tot} = -0.71	q_{Bi} = 1.95, q_O = -1.18, q_{tot} = 0.77
L12	q_{Bi} = 1.97, q_O = -0.98, q_{tot} = 0.99	q_{Fe} = 1.74, q_O = -0.76, q_{tot} = 0.22

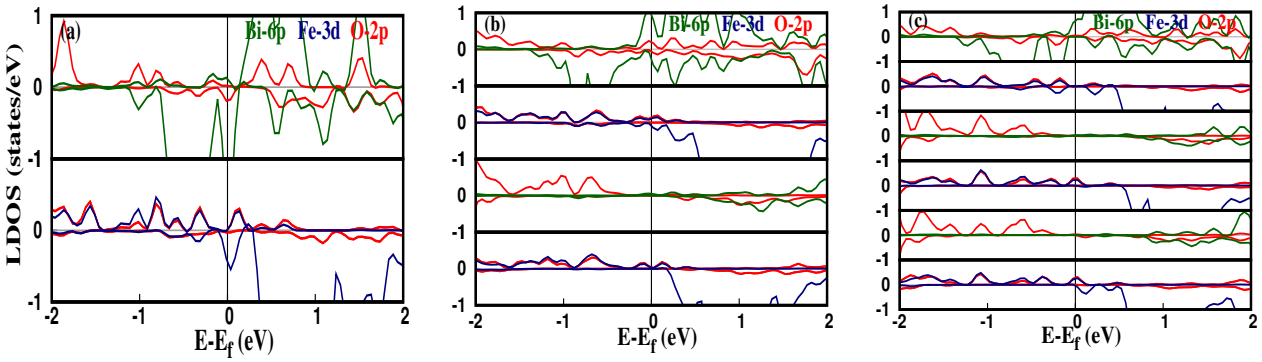

Fig. 3 Local density of states (LDOS) of structure-II with BiO terminated surface thickness of (a) 2L, (b) 4L and (c) 6L respectively.

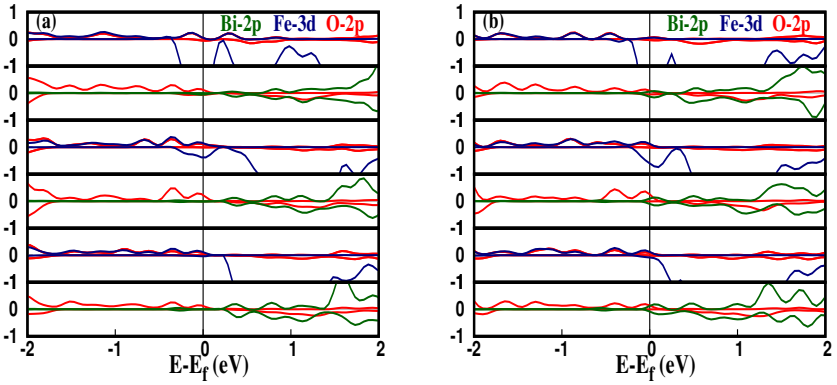

Fig. 4 Local density of states (LDOS) of 6L slab-thicknesses with FeO_2 termination for (a) structure-III and (b) structure-IV respectively.

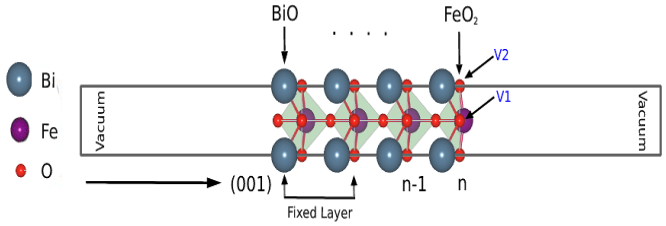

Fig. 5 Oxygen vacancy on the 4L thick FeO_2 terminated surface with at site-1 (V1) , and at site-2 (V2) respectively.

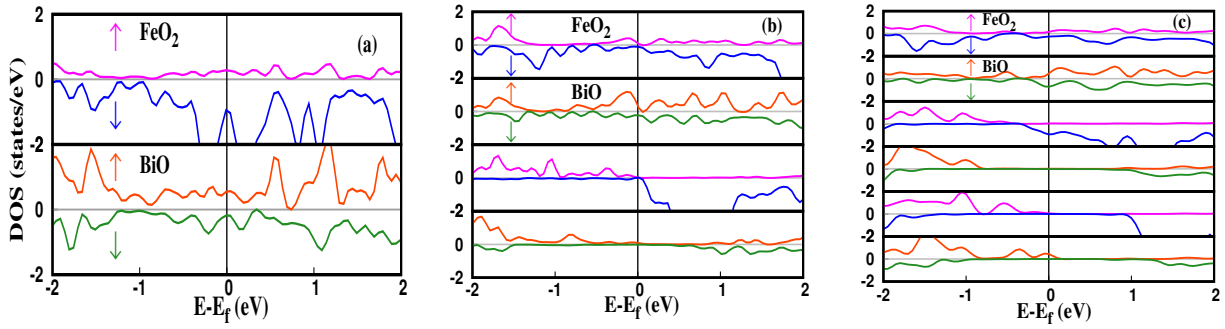

Fig. 6 Layered density of states (DOS) corresponding to Structure-II with oxygen vacancy at 'V1' site on FeO_2 terminated surface thickness of (a) 2L, (b) 4L and (c) 6L respectively.

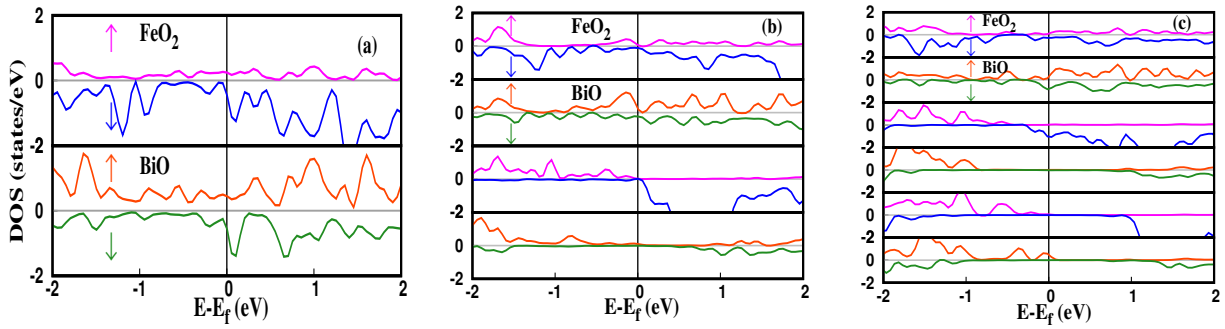

Fig. 7 Layered density of states (DOS) corresponding to Structure-II with oxygen vacancy at 'V2' site on FeO_2 terminated surface thickness of (a) 2L, (b) 4L and (c) 6L respectively.

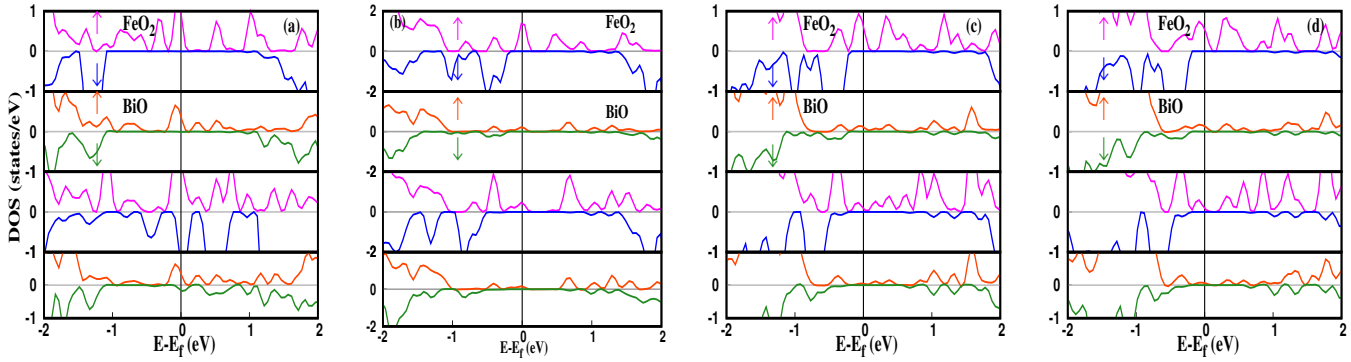

Fig. 8 Density of states (DOS) of 4L slab-thicknesses with FeO_2 termination for (a) structure-I, (b) structure-II, (c) structure-III, and (d) structure-IV respectively.

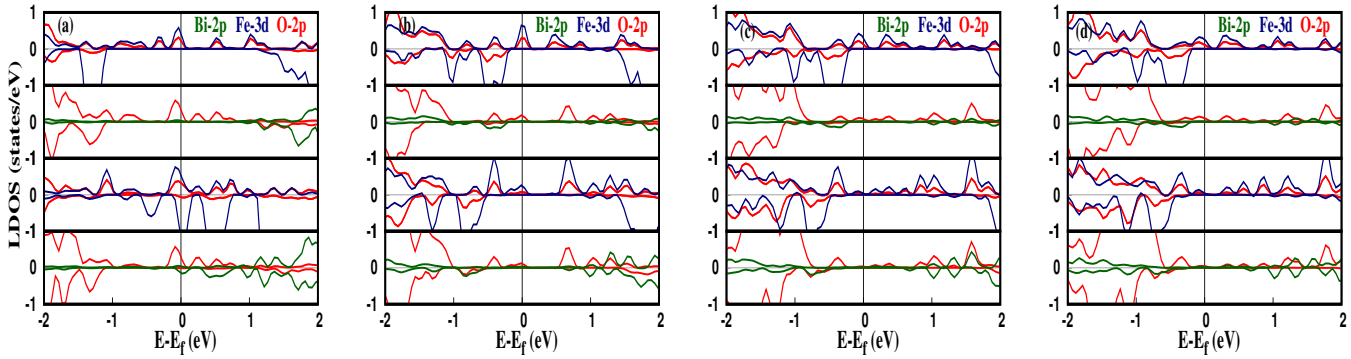

Fig. 9 Local density of states (LDOS) of 4L slab-thicknesses with FeO_2 termination for (a) structure-I, (b) structure-II, (c) structure-III, and (d) structure-IV respectively.

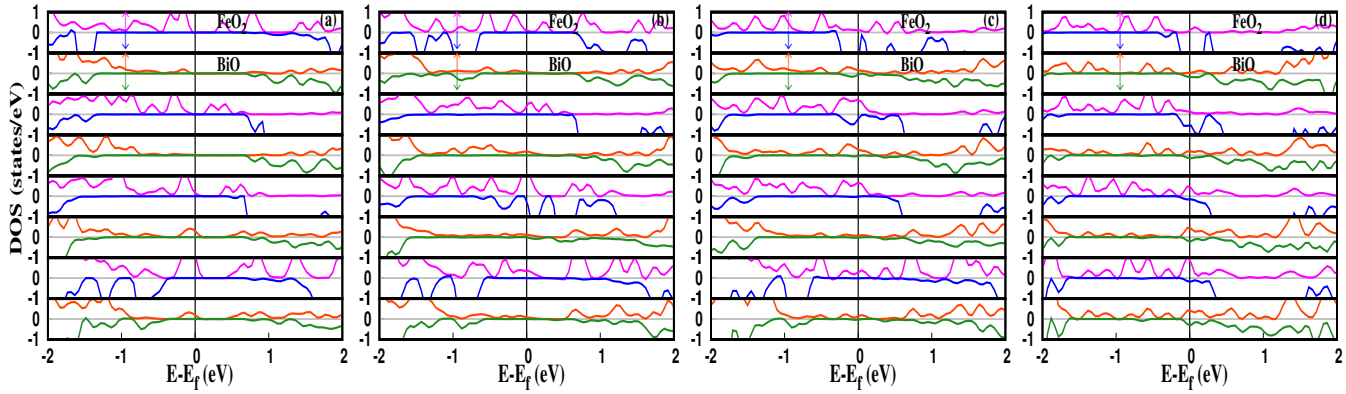

Fig. 10 Density of states (DOS) of 8L slab-thicknesses with FeO_2 termination for (a) structure-I, (b) structure-II, (c) structure-III, and (d) structure-IV respectively.

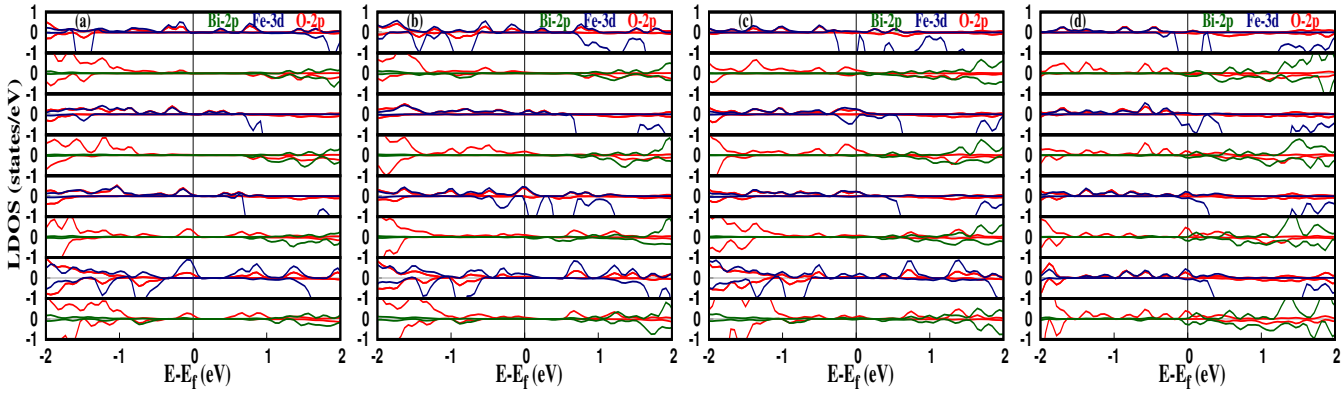

Fig. 11 Local density of states(LDOS) of 8L slab-thicknesses with FeO_2 termination for (a) structure-I, (b) structure-II, (c) structure-III, and (d) structure-IV respectively.

Table 2 The angle $O_e - Fe - O_e$ (in deg)(where O_e is the equatorial oxygen O2/O3), angle $O1 - Fe - O1$ (in deg)(where O1 is the axial oxygen), the bond-length O1-Fe (in Å)and the Fe-O_e bond-length (in Å) are presented for fixed layer(FL), 2L, 4L and 6L belonging to structures I, II, III and IV, respectively.

	FL	2L	4L	6L
Structure-I				
$O_e - Fe - O_e(\theta_1)$	146.85	157.50	158.59	158.70
$O1 - Fe - O1(\theta_2)$	180.00	180.00	180.00	180.00
O1-Fe	2.23	2.73	2.67	2.68
			2.74	2.68
				2.74
O_e-Fe	1.91	1.87	1.87	1.87
Structure-II				
$O_e - Fe - O_e(\theta_1)$	147.70	166.34	168.17	171.43
$O1 - Fe - O1(\theta_2)$	180.00	180.00	180.00	180.00
O1-Fe	2.30	2.46	2.37	2.27
			2.47	2.46
				2.52
O_e-Fe	1.96	1.90	1.90	1.89
Structure-III				
$O_e - Fe - O_e(\theta_1)$	161.19	178.78	178.28	178.28
$O1 - Fe - O1(\theta_2)$	180.00	180.00	180.00	180.00
O1-Fe	2.11	1.94	1.98	1.97
			2.09	2.08
				2.08
O_e-Fe	1.97	1.94	1.94	1.94
Structure-IV				
$O_e - Fe - O_e(\theta_1)$	162.67	179.91	179.32	179.56
$O1 - Fe - O1(\theta_2)$	180.00	180.00	180.00	180.00
O1-Fe	2.12	1.89	1.91	1.91
			2.01	2.00
				2.00
O_e-Fe	1.99	1.97	1.97	1.97

Table 3 The magnetic moment (M in μ_B) of 'Fe' in the FeO_2 plane of the slab structures.

Structures	2L	4L	6L
I	3.04	3.04	3.04
	3.52	3.65	3.65
		3.62	3.69
		3.48	3.64
			3.63
			3.47
II	2.99	2.97	2.96
	3.57	3.72	3.73
		3.67	3.72
		3.53	3.68
			3.65
			3.51
III	2.93	2.94	3.38
	3.60	3.77	3.75
		3.73	3.79
		3.60	3.78
			3.77
			3.61
IV	2.94	2.94	3.53
	3.58	3.75	3.77
		3.72	3.77
		3.58	3.77
			3.75
			3.60

and (c)), we can observe that the Fe-3d orbital contributes to these electron carriers.

Table 4 Spin-polarized charge corresponding to structure-II.

	FeO_2 termination
Layer-No.	Two-layers (2L)
L1	Fe ↑=9.17,Fe ↓=5.38,O ↑=3.56,O ↓=3.61
L2	Bi ↑=6.61,Bi ↓=6.61,O ↑=3.67,O ↓=3.54
L3	Fe ↑=9.30,Fe ↓=4.94,O ↑=3.65,O ↓=3.56
L4	Bi ↑=6.54,Bi ↓=6.51,O ↑=3.30,O ↓=3.68
	Four-layers (4L)
L1	Fe ↑=9.13,Fe ↓=5.40,O ↑=3.55,O ↓=3.61
L2	Bi ↑=6.60,Bi ↓=6.60,O ↑=3.70,O ↓=3.51
L3	Fe ↑=9.35,Fe ↓=4.84,O ↑=3.66,O ↓=3.55
L4	Bi ↑=6.60,Bi ↓=6.57,O ↑=3.70,O ↓=3.54
L5	Fe ↑=9.34,Fe ↓=4.88,O ↑=3.68,O ↓=3.56
L6	Bi ↑=6.55,Bi ↓=6.54,O ↑=3.71,O ↓=3.51
L7	Fe ↑=9.29,Fe ↓=5.00,O ↑=3.62,O ↓=3.58
L8	Bi ↑=6.52,Bi ↓=6.52,O ↑=3.56,O ↓=3.42
	Six-layers (6L)
L1	Fe ↑=9.11,Fe ↓=5.40,O ↑=3.55,O ↓=3.60
L2	Bi ↑=6.60,Bi ↓=6.60,O ↑=3.73,O ↓=3.52
L3	Fe ↑=9.33,Fe ↓=4.83,O ↑=3.67,O ↓=3.54
L4	Bi ↑=6.59,Bi ↓=6.56,O ↑=3.74,O ↓=3.50
L5	Fe ↑=9.33,Fe ↓=4.85,O ↑=3.67,O ↓=3.55
L6	Bi ↑=6.59,Bi ↓=6.57,O ↑=3.70,O ↓=3.54
L7	Fe ↑=9.35,Fe ↓=4.88,O ↑=3.68,O ↓=3.56
L8	Bi ↑=6.55,Bi ↓=6.54,O ↑=3.74,O ↓=3.49
L9	Fe ↑=9.34,Fe ↓=4.91,O ↑=3.67,O ↓=3.55
L10	Bi ↑=6.55,Bi ↓=6.54,O ↑=3.74,O ↓=3.46
L11	Fe ↑=9.30,Fe ↓=5.02,O ↑=3.61,O ↓=3.58
L12	Bi ↑=6.52,Bi ↓=6.52,O ↑=3.61,O ↓=3.37

Table 5 Estimation of the surface energies(in unit J/m^2) for the FeO_2 surface termination.

Structures	str-I	str-II	str-III	str-IV
4L	0.01	1.4	2.69	2.82
6L	-2.25	0.50	3.09	1.98